

Supporting information

Redox-dual-sensitive multiblock copolymer vesicles with disulfide-enabled sequential drug delivery†

Cheng Cheng, ‡^{ab} Jiayun Ma, ‡^{ab} Jinling Zhao,^b Haiying Lu,^a Yang Liu,^b Chuanshi He,^c Man Lu,^c Xiaohong Yin,^{*a} Jianshu Li,^b Mingming Ding^{*b}

^aScience and Technology Innovation Center, Guangyuan Central Hospital, Guangyuan 628000, China.

^bCollege of Polymer Science and Engineering, State Key Laboratory of Polymer Materials Engineering, Sichuan University, Chengdu 610065, China.

^cDepartment of Ultrasound Medical Center, Sichuan Cancer Hospital and Institute, Sichuan Cancer Center, School of Medicine, University of Electronic Science and Technology of China, Chengdu.

* Corresponding Authors.

‡ These authors contributed equally to this paper.

Materials

Polyethylene glycol (PEG, MW 2000) was purchased from J&K Scientific Ltd. (Shanghai, China). Polycaprolactone (PCL, 99%, MW 2000) was obtained from Daicel Chemical Industries, Ltd. (Japan). Rhodamine 6G (R6G, 95%) and nile red (NR) were obtained from TCI (Tokyo, Japan). 30% hydrogen peroxide (H₂O₂) was purchased from Chengdu Kelong Chemical Co., Ltd. Doxorubicin hydrochloride (DOX·HCl) was purchased from Meilun Biotech Co., Ltd. Glutathione (GSH) was purchased from Biofroxx (Einhausen, German). Paclitaxel (PTX, 99.5%) was obtained from Shanghai Jinhe Bio-Technology Co., Ltd., China. High glucose culture fluid, trypsin, penicillin/streptomycin and bovine serum albumin (BSA) were purchased from Gibco. Dichlorodihydrofluorescein Diacetate (DCFH-DA) was obtained from Adamas Reagent, Ltd. (Shanghai, China). Calcein-AM/propidium iodide (PI) double stain kit was supplied by Solarbio (Beijing, China). The cell counting kit-8 (CCK-8) was purchased from Sigma. Calreticulin rabbit monoclonal antibody (cat. no. AF1666) and fluorescein isothiocyanate (FITC)-labeled Goat Anti-Rabbit IgG (H+L) (cat. no. A0562) were obtained from Beyotime Institute of Biotechnology (Shanghai, China). 4',6-Diamidino-2-phenylindole (DAPI) was supplied by Sigma (St. Louis, MO, USA). Other reagents unless specified were

obtained from commercial suppliers and used without further purification.

Instruments and measurements

The chemical structures of copolymers were confirmed by ^1H -nuclear magnetic resonance (^1H NMR) performed on a Varianunity Inova-400 spectrometer (400 MHz, USA). The samples were dissolved in CDCl_3 and the internal standard was tetramethylsilane (TMS).

The molecular weight of copolymer was characterized by gel permeation chromatography (GPC, TOSOH Corporation, Japan) with Tetrahydrofuran (THF) as the mobile phase and polystyrene as a standard. The sample concentration was 2 mg mL^{-1} and the flow rate was 1.0 mL min^{-1} .

Fourier transform infrared (FTIR) spectra were recorded on a Nicolet iS10 spectrometer (Thermo Electron Corporation, USA) from $4\,000$ to 600 cm^{-1} with a transmission mode. Before measurement, the low-concentration samples dissolved in dichloromethane were dropped on a clean KBr wafer. After removal of solvent, the wafer was placed in a $70 \text{ }^\circ\text{C}$ oven for 6 h, and then cooled at room temperature for 48 h under argon protection.

The size and size distribution of copolymers were measured on a Zetasizer Nano ZS90 instrument (Malvern Instruments Ltd., UK) at an angle of 90° . All datas were calculated as mean \pm standard deviation (SD) based on triplicate independent experiments.

UV-vis absorption spectra were obtained using a UV2600 spectrophotometer (Techcomp, Ltd., China) and a quartz cuvette having an optical path length of 1.00 cm. Depending on the samples, the same solvent as sample solution was used for background subtraction.

Fluorescence measurement was conducted on an F-4600 FL spectrophotometer (Hitachi, Ltd., Japan). For R6G, the emission spectra were collected from 500 to 700 nm at excitation wavelength (λ_{em}) of 526 nm. For DOX·HCl, the emission spectra were collected from 500 to 800 nm at excitation wavelength (λ_{em}) of 488 nm. For NR, the emission spectra were collected from 550 to 800 nm at excitation wavelength (λ_{em}) of 530 nm.

The morphology of self-assemblies was confirmed by dynamic light scattering (DLS) on

a Brookhaven Instruments BI-200SM goniometer with a BI-9000 correlator and static light scattering (SLS) measurements on a Spectra Physics Millennia-II diode with laser light of wavelength 532 nm. The concentration of the samples was 0.2 mg mL⁻¹. All the samples were filtered through a 0.45 µm Millipore filter (PVDF) before measurement. The detection angles were 30°, 45°, 60°, 75°, 90° for DLS test and 45°, 60°, 75°, 90°, 105°, 120°, 135° for SLS test. All data were obtained as mean ± standard deviation (SD) based on triplicate independent experiments. The radii of gyration (R_g) was obtained from CONTIN analyses of DLS measurements and the mean hydrodynamic radii (R_h) was resulted from SLS measurements.

The morphologies of copolymers were further visually observed by transmission electron microscope (TEM). The samples were placed on a copper grid with Formvar film and stained with 1% (w/v) phosphotungstic acid for 4 min before measurements. Excess samples were sponged with a filter paper. The specimen was air-dried and scanned using a transmission electron microscope (H-600-4, Hitachi, Ltd., Japan), operating at an accelerating voltage of 75 kV at room temperature (25 °C).

X-ray photoelectron spectroscopy (XPS) analysis was used to evaluate the element valence and quantity changes. It was carried out on a K-Alpha spectrometer (Thermo Fisher Scientific Inc.) equipped with a monochromatic Al K α X-ray source operated at 12 kV.

High-performance liquid chromatography (HPLC) was operated on a 1260 Infinity (Agilent Technologies, USA) equipped with an Eclipse Plus C18 column (4.6×150 mm), using a mixture of acetonitrile (60%) and H₂O (40%) as the eluent. The flow rate of the mobile phase was 1.0 mL min⁻¹. All the aqueous samples were passed through a 0.45 µm pore-sized syringe filter (Millipore, Carrigtwohill, Co. Cork, Ireland).

Synthesis and oxidation of multiblock copolymers (MCP)

PEG (6.0 g) and PCL (6.0 g) were dissolved in 60 mL anhydrous dichloroethane (DCE) in a flask. Then, 2.1 g L-cystine dimethyl ester diisocyanate (CDI) and 0.1% stannous octoate was added under a dry argon atmosphere for 24 h of reaction at 60 °C, and continued at 80 °C

for additional 24 h. Then reaction system was condensed by evaporation and precipitated in ice diethyl ether for three times to give a white solid (72% yield). The structure of MCP was characterized by ^1H NMR. As shown in Figure S1, the peaks at 4.06 ($-\text{CH}_2\text{O}-$), 2.31 ($-\text{CH}_2\text{COO}-$), 1.64 ($-\text{CH}_2\text{CH}_2\text{CH}_2-$) and 1.38 ($-\text{CH}_2\text{CH}_2\text{CH}_2-$) ppm are ascribed to the methylene protons of PCL segment. The peak at 3.64 ppm ($-\text{CH}_2\text{CH}_2\text{O}-$) is assigned to the methylene groups of PEG block. The chemical shifts of methylene and methyl groups of CDI residue are at 3.18 and 3.77 ppm ($-\text{CH}_2-\text{S}-$, $\text{CH}_3\text{O}-$). GPC test indicates that the weight average molecular weights of MCP are 25911 g mol^{-1} , with narrow molecular weight distributions (PDI 1.62, Figure S2). These results demonstrate that MCP was synthesized successfully. The copolymers were later treated with 500 mM H_2O_2 and named as MCP-O.

Self-assembly of copolymers

The polymeric assemblies were prepared via a dialysis method. Briefly, solutions of copolymer (10 mg) in 1 mL *N,N*-dimethylacetamide (DMAC) were added dropwise to 8 mL deionized water with quickly stirring. Then the solutions were dialyzed in a dialysis bag (retained molecular weight: 3500 Da) dialyzed for 2 d, changing the external water once 4 h. Finally, the solutions were centrifugalized for 15 min at 3000 r min^{-1} and filtered through a $0.45 \mu\text{m}$ pore-sized syringe filter (Millipore, Carrigtwohill, Co. Cork, Ireland).

Encapsulation of DOX·HCl and R6G

To ensure the confinement of the hydrophilic dye into the water-filled interior of the vesicles, two hydrophilic dyes DOX·HCl and R6G were incorporated into the nanostructures. MCP and MCP-O copolymers (6 mg) in DMAC (1 mL) were added dropwise (30 s d^{-1}) into an aqueous solution (6 mL) containing 0.33 mg DOX·HCl or R6G. After stirring in the dark for 30 min, the solutions were dialyzed in a dialysis bag (retained molecular weight: 3500 Da) for 2 d, changing the external water once 4 h. Finally, the solutions were centrifugalized for 15 min at 3000 r min^{-1} and filtered through a $0.45 \mu\text{m}$ pore-sized syringe filter (Millipore, Carrigtwohill, Co. Cork, Ireland). As a control, DOX·HCl and R6G were dissolved in deionized water to attain

aqueous solutions. The UV-vis spectra were taken and the concentrations of free DOX·HCl and R6G in water was adjusted so that the UV-vis absorption matched the intensity of DOX·HCl and R6G encapsulated in assemblies (Fig. 2C). The fluorescence emission spectra were recorded on an F-4600 FL spectrophotometer at a λ_{ex} of 480 nm (DOX·HCl) or 526 nm (R6G).

Encapsulation of NR

A mixture of NR (0.1 mg) and copolymers (6 mg) in DMAC (1 mL) was added dropwise (30 s d^{-1}) into 6 mL aqueous solution. After stirring in the dark for 30 min, the solutions were dialyzed in a dialysis bag (retained molecular weight: 3500 Da) for 2 d, changing the external water once 4 h. Finally, the solutions were centrifugalized for 15 min at 3000 r min^{-1} and filtered through a $0.45 \mu\text{m}$ pore-sized syringe filter (Millipore, Carrigtwohill, Co. Cork, Ireland). The fluorescence emission spectra were recorded on an F-4600 FL spectrophotometer at a λ_{ex} of 530 nm.

Oxidation-responsive drug release

The release of DOX·HCl and NR from copolymer vesicles was studied using a fluorescent technique. The DOX·HCl- or NR-encapsulated vesicles (1.8 mL) were placed in a quartz cuvette and stimulated by 5 M H_2O_2 (0.2 mL) in situ. As a control, the DOX·HCl- or NR-encapsulated vesicles were treated with equivalent volume of deionized water. The fluorescence emission spectra of samples were tested at different time points.

For DOX·HCl, the excitation wavelength was 488 nm and the emission wavelength was in the range of 500-800 nm, the release rates at different time points can be calculated by $(I_t - I_0) / (I_{\text{free}} - I_0) \times 100\%$ as a function of time (h), where I_0 is the fluorescence intensity at the initial time, I_t is the fluorescence intensity of DOX·HCl at different time points, I_{free} is the fluorescence intensity of free DOX·HCl dissolved in water with the same concentration as that encapsulated in vesicles.

For NR, the excitation wavelength was 530 nm and the emission wavelength ranged from

550 to 800 nm, the release rates at different time points can be calculated by $(I_0 - I_t) / I_0 \times 100\%$ as a function of time (h), where I_0 is the fluorescence intensity at the initial time, I_t is the fluorescence intensity of NR at different time points.

Reduction-responsive drug release

The NR-encapsulated vesicles (1.8 mL) were placed in a quartz cuvette and stimulated by 10 mM GSH in situ. The fluorescence emission spectra were recorded at different time points. The release rates at different time points were calculated by $(I_0 - I_t) / I_0 \times 100\%$ as a function of time (h), where I_0 is the fluorescence intensity at the initial time, I_t is the fluorescence intensity of NR at different time points.

Photo-responsive drug release

For DOX·HCl encapsulation, a mixture of IR780 (3 mg) and copolymers (6 mg) in DMAC (1 mL) was added dropwise (30 s d^{-1}) into 6 mL aqueous solution containing DOX·HCl (2 mg) under stirring. For NR encapsulation, a mixture of IR780 (3 mg), NR (0.04 mg) and copolymers (6 mg) in DMAC (1 mL) was added dropwise (30 s d^{-1}) into 6 mL aqueous solution under stirring. After stirring in the dark for 30 min, the two solutions were respectively dialyzed in a dialysis bag (retained molecular weight: 3500 Da) for 2 d, changing the external water once 4 h. Finally, the solutions were centrifugalized for 15 min at 3000 r min^{-1} and filtered through a $0.45 \mu\text{m}$ pore-sized syringe filter (Millipore, Carrigtwohill, Co. Cork, Ireland). To track the drug release under oxidative conditions, the two solutions were placed in a quartz cuvette respectively and irradiated with 808 nm laser at 2 W cm^{-2} for 5 min. The fluorescence emission spectra were recorded on an F-4600 FL spectrophotometer at λ_{ex} of 488 nm (DOX·HCl) or 530 nm (NR) at different time points after 5 min of irradiation. The release rate of DOX·HCl at different time points was calculated by $(I_t - I_0) / (I_{\text{free}} - I_0) \times 100\%$ as a function of time (h), where I_0 is the initial fluorescence intensity, I_t is the fluorescence intensity of DOX·HCl at different time points after irradiation, I_{free} is the fluorescence intensity of free DOX·HCl dissolved in water with the same concentration as that encapsulated in vesicles. The release rate of NR at

different time points was calculated by $(I_0 - I_t) / I_0 \times 100\%$ as a function of time (h), where I_0 is the initial fluorescence intensity, I_t is the fluorescence intensity of NR at different time points after irradiation.

Preparation of DOX·HCl- and PTX-loaded polymersomes

A mixture of IR780, PTX and copolymers (6 mg) in DMAC (1 mL) was added dropwise ($1 \text{ d } 30\text{s}^{-1}$) into 6 mL aqueous solution containing DOX·HCl under stirring. After stirring in the dark for 30 min, the solutions were dialyzed in a dialysis bag (retained molecular weight: 3500 Da) for 2 d, changing the external water once 4 h. Finally, the solutions were centrifugalized for 15 min at 3000 r min^{-1} and filtered through a $0.45 \mu\text{m}$ pore-sized syringe filter (Millipore, Carrigtwohill, Co. Cork, Ireland). The loading content of DOX·HCl was determined by an F-4600 FL spectrophotometer (Hitachi, Ltd., Japan). The loading content of PTX was determined by high-performance liquid chromatography (HPLC, 1260 Infinity, Agilent Technologies, USA) equipped with an Eclipse Plus C18 column ($4.6 \times 150 \text{ mm}$).

Cytotoxicity assay

A CCK-8 assay was performed to evaluate the cytocompatibility or cytotoxicity of different samples. Briefly, 3T3 cells or GL261 cells were seeded in 96-well plates at a density of 5×10^3 cells per well and cultured overnight. To estimate the cytocompatibility of drug-free vesicles, the 3T3 or GL261 cells were treated with fresh medium containing a known concentration of drug-free vesicles ranging from 12.5 to $800 \mu\text{g mL}^{-1}$ in each well in triplicates. To estimate the cytotoxicity of DOX·HCl and PTX administrated concurrently or sequentially, the GL261 cells were treated with fresh medium containing the DOX·HCl and PTX in each well in triplicates for 24 h (concurrent group), or the GL261 cells were first treated with fresh medium containing DOX·HCl for 6 h and then additional PTX for further 18 h (sequential group) in each well in triplicates. To evaluate the cytotoxicity of drug-loaded nanoreactors, the GL261 cells were treated with fresh medium containing drug-loaded nanoreactors at different DOX·HCl and PTX concentrations ($C_{\text{DOX}\cdot\text{HCl}} : C_{\text{PTX}} : C_{\text{IR780}} = 3:1:1.5$) after 3 min of irradiation

with 808 nm laser (2 W cm^{-2}) in each well in triplicates for 24 h. The above cells were finally processed with CCK-8 solution (10 μL) for another 1-4 h. The absorbance of each sample was recorded at 450 nm using a microplate reader (DNM-9602, Nanjing Perlove Medical Equipment Co., Ltd., China). The cell viability was calculated by $(A_s - A_b) / (A_c - A_b)$, where A_s represents the absorbance of the experimental cells, A_b represents the absorbance of background, A_c represents the absorbance of control cells.

Live/dead cells staining assay

To further affirm the cytotoxicity, we used live/dead double staining kit to detect the viable and dead cells (viable cells stain with green and dead cells stain with red). Briefly, the GL261 cells (1×10^5) were seeded in 48-well plates overnight at 37 °C. Afterward, drug-loaded nanoreactors were added to each well in triplicates, followed by 3 min of laser irradiation (808 nm, 2 W cm^{-2}). After incubation for 24 h, the cells were treated with Calcein-AM/PI for 20 min and analyzed with a Leica microsystem (DMi 8).

Detection of ROS generation

As a fluorescent probe for ROS in cells, DCFH-DA was non-fluorescent before penetrating into cells. The diacetate group of DCFH-DA would be removed by intracellular esterases after entering the cells. The remaining part would be oxidized rapidly and emit green fluorescence in the presence of ROS. Based on this principle, GL261 cells were co-incubated with drug-loaded nanoreactors ($C_{\text{IR780}}: 2 \mu\text{g mL}^{-1}$) overnight in 96 well plates. Subsequently, DCFH-DA (50 μM) was added to each well and incubated with the cells for 20-30 min. Finally, the cells were washed with PBS and then exposed to 808 nm laser irradiation (2 W cm^{-2}) for 3 min. Fluorescence images in the irradiation regions were immediately captured on a Leica microsystem (DMi 8) using an excitation of 488 nm.

Calreticulin (CRT) exposure

For immunofluorescent staining, drug-loaded nanoreactors were added to the GL261 cells planted on the glass slide and irradiated with 808 nm laser (2 W cm^{-2}) for 3 min. After 24 h

incubation, the cells were washed with PBS for three times and fixed with polyformaldehyde for 15 min. Afterwards, the cells were stained with calreticulin rabbit monoclonal antibody for 1.5 h and FITC-labeled secondary antibody for 1 h. Finally, the cells were stained with DAPI and captured using a confocal laser scanning microscopy (CLSM, Zeiss, LSM710).

Computational simulation

Dissipative particle dynamics (DPD) simulation was used to investigate the self-assemble configurations of MCP and MCP-O copolymers. DPD simulation method was developed by Hoogerbrugge and Koelman¹ in 1992 and was further improved by Español and Warren² in 1995. The soft-core DPD bead represent a group of atoms and the force between them is defined by three additive components:

$$f_i = \sum_{j \neq i} (F_{ij}^C + F_{ij}^D + F_{ij}^R) \quad (S1)$$

where F_{ij}^C , F_{ij}^D and F_{ij}^R represent conservative, dissipative, and random forces, respectively. The dissipative force F_{ij}^D is a friction force that reduces the velocity differences between DPD beads, and the random force F_{ij}^R compensates the loss of energy due to the dissipative force and reduce the relative momentum.

The conservative force is defined as:

$$F_{ij}^C = \begin{cases} \alpha_{ij}(1 - r_{ij}) \hat{r}_{ij}, & r_{ij} < 1 \\ 0, & r_{ij} > 1 \end{cases} \quad (S2)$$

where α_{ij} and r_{ij} are the repulsive interaction parameter and distance between particles i and j . \hat{r}_{ij} is the unit vector joining beads i and j .

$$a_{ij} \approx 25 + 3.27\chi_{ij} \quad (S3)$$

χ_{ij} is the Flory-Huggins parameter and defined as:

$$\chi_{ij} = \frac{(\delta_j - \delta_i)V_r}{RT} \quad (S4)$$

$$V_r = \min(V_j, V_i) \quad (S5)$$

Where δ_j and V_r are the Hansen solubility parameter and the reference volume. The solubility parameters used in our simulation are listed in Table S1.

The polymer chains are represented by bead-spring models where the harmonic bond potential is:

$$E_{bond} = 0.5k_b (r - r_0)^2 \quad (S6)$$

Here $k_b = 128$ is the elastic bond strength, and $r_0 = 0.5$ is the equilibrium bond distance³.

We carried out the simulation with LAMMPS software package⁴ and the snapshots are rendered in VMD⁵. The periodic boundary condition was applied on a cubic simulation box of $40 \times 40 \times 40r_c^3$ to eliminate the finite size effects. The bead density of the system ($\rho = 3$) is close to that of water and the cutoff radius is the unit length $r_c = 1$. A time step of 0.02 was adopted and the simulation lasted for 3,000,000 steps. 390 MCP or MCP-O polymers are added into the system, as shown in the snapshots of Figure 1E.

The bond energy and length calculation

Density functional theory (DFT) calculations were carried out in order to compute and compare the bond energy and length of the disulfide linkages in MCP and MCP-O polymers. The molecular structures were optimized by the B3LYP functional^{6,7} at the levels of the 6-31G(d) basis set⁸. The SMD solvent model⁹ was used. We carried out the simulation using ORCA 4.0.0.2 program package¹⁰.

Statistical analysis

The quantitative data obtained were expressed as means \pm standard deviations (SD). Statistical analysis was carried out using the Statistical Package for the Social Sciences (IBM SPSS Statistics software, Version 19, IBM, New York, USA). Student's t-test or one-way analysis of variance (ANOVA) was performed to determine the statistical significance within the data at 95% confidence levels ($P < 0.05$).

Supporting Figures and Tables

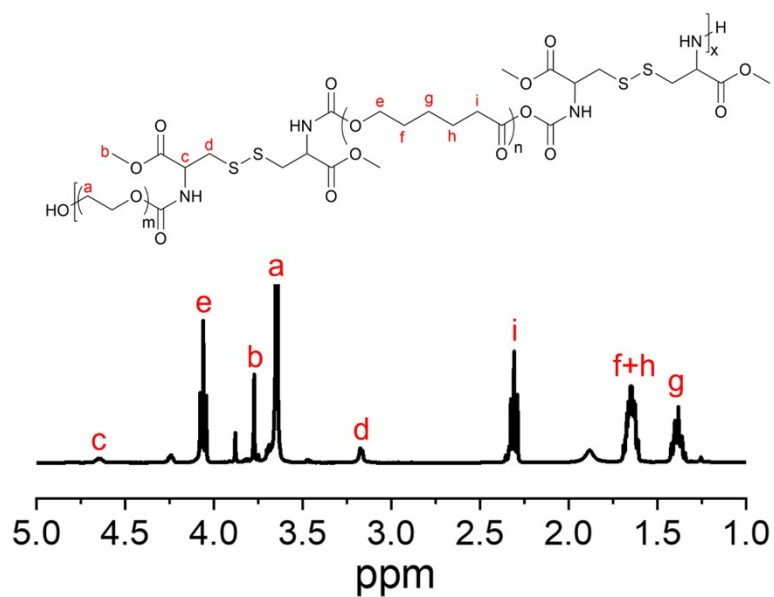


Fig. S1 400 MHz ^1H NMR spectrum of MCP in CDCl_3 .

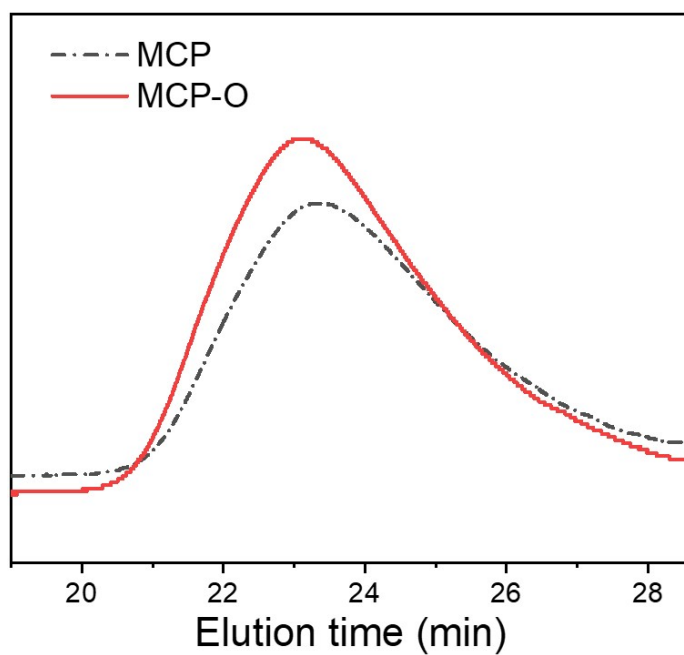


Fig. S2 GPC spectra of MCP and MCP-O in THF.

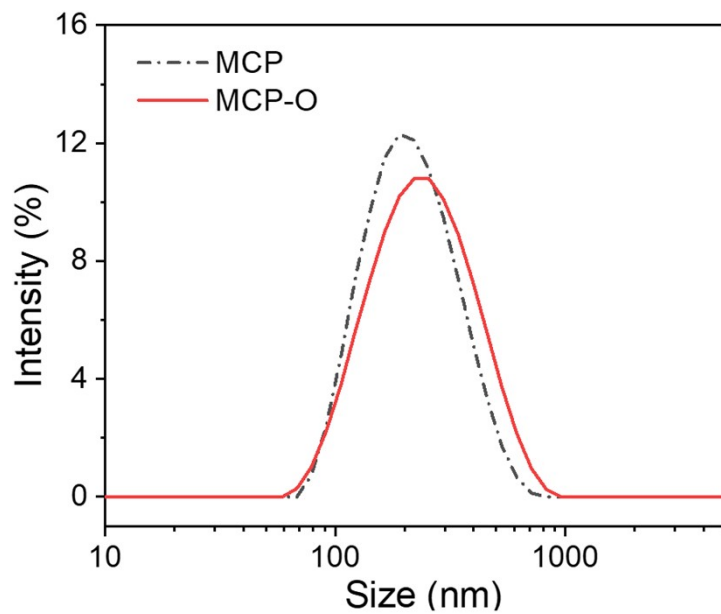


Fig. S3 Size distribution curves of MCP and MCP-O assemblies determined by DLS.

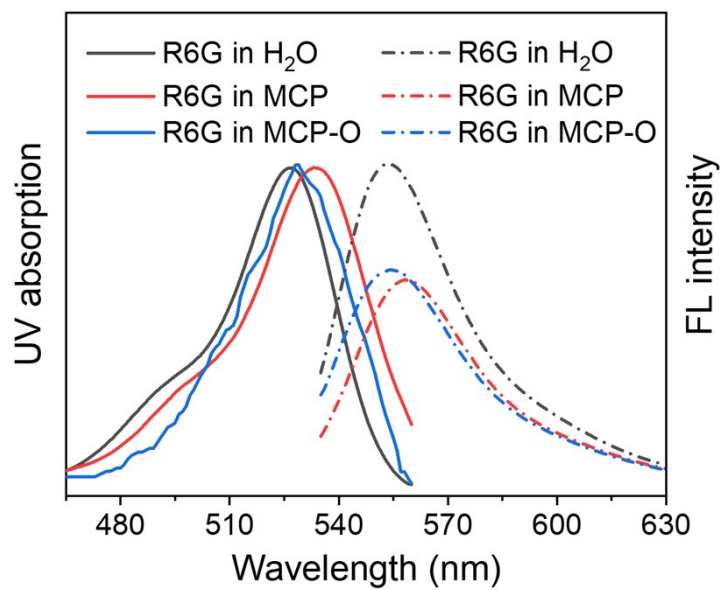


Fig. S4 UV-vis spectra (left) and fluorescence emission spectra ($\lambda_{\text{ex}} = 526$ nm, right) of R6G in H₂O, MCP and MCP-O assemblies.

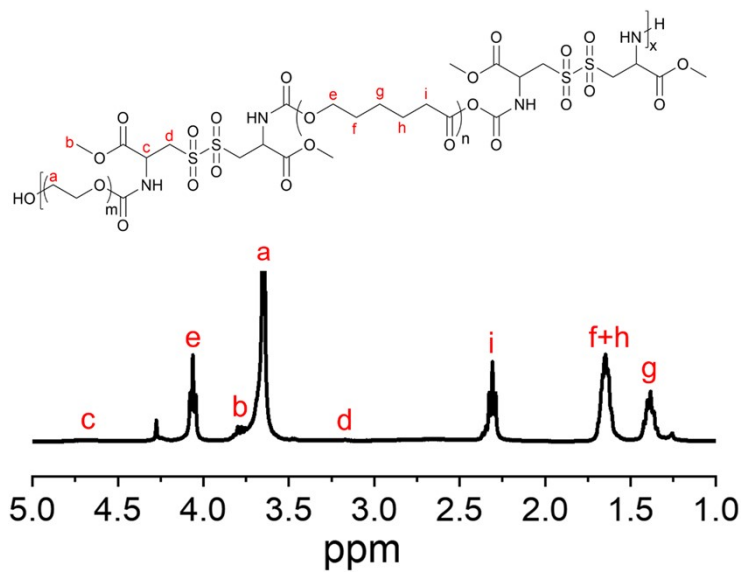


Fig. S5 400 MHz ^1H NMR spectrum of MCP-O in CDCl_3 .

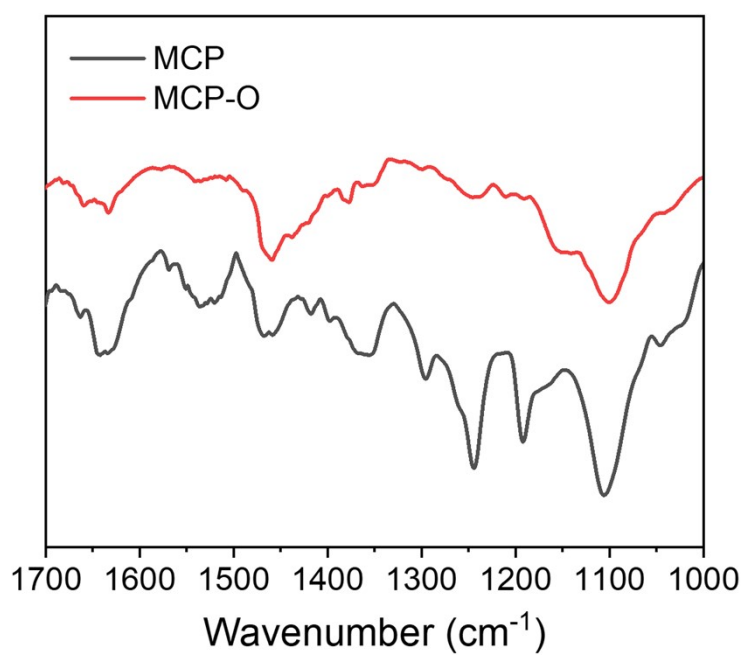


Fig. S6 FTIR spectra of MCP and MCP-O (1000-1700 cm^{-1}).

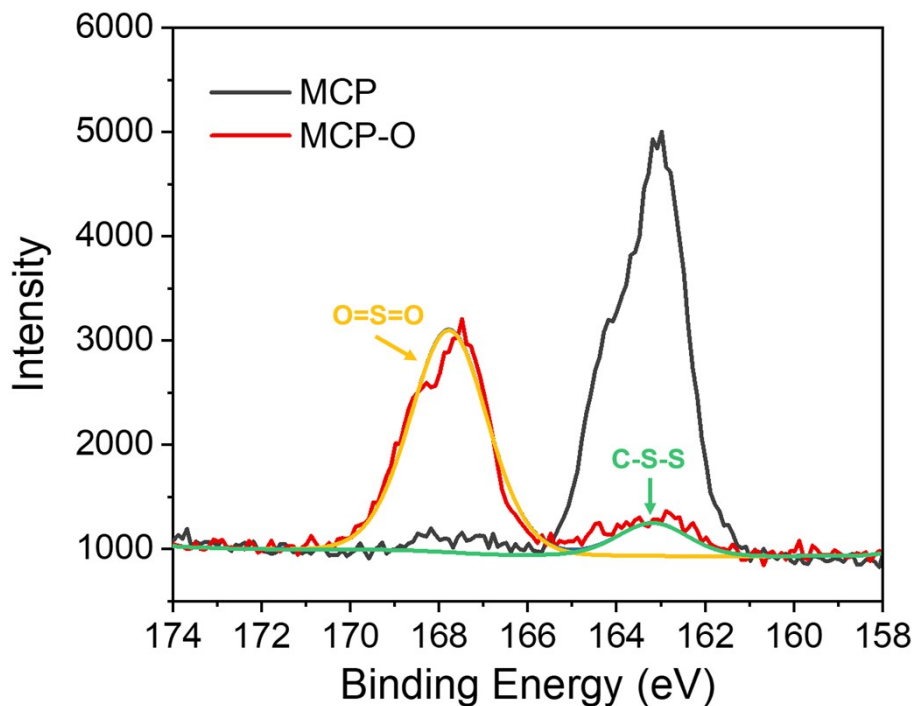


Fig. S7 XPS spectra of sulfur of MCP before and after oxidation in the binding energy range of 158-174 eV.

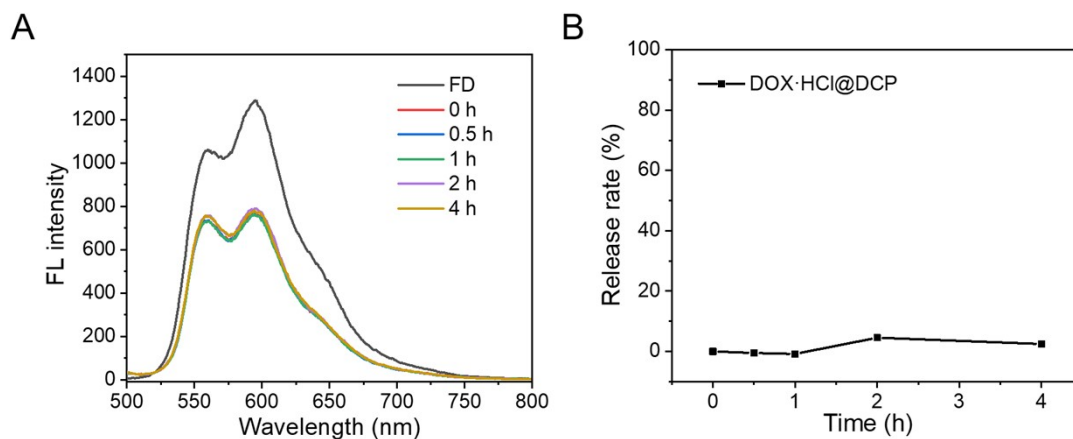


Fig. S8 Fluorescence spectra (A) and release rates (B) of DOX·HCl-encapsulated DCP incubated with 500 mM H_2O_2 for different time. FD represents free DOX·HCl in an aqueous solution, with the same concentration of that encapsulated in vesicles.

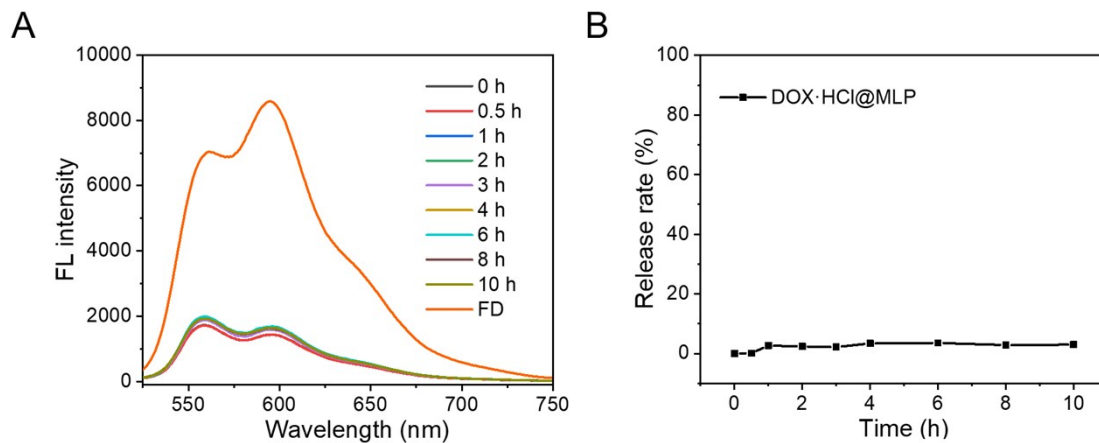


Fig. S9 Fluorescence spectra (A) and release rates (B) of DOX·HCl-encapsulated MLP incubated with 500 mM H₂O₂ for different time. FD represents free DOX·HCl in an aqueous solution, with the same concentration of that encapsulated in vesicles.

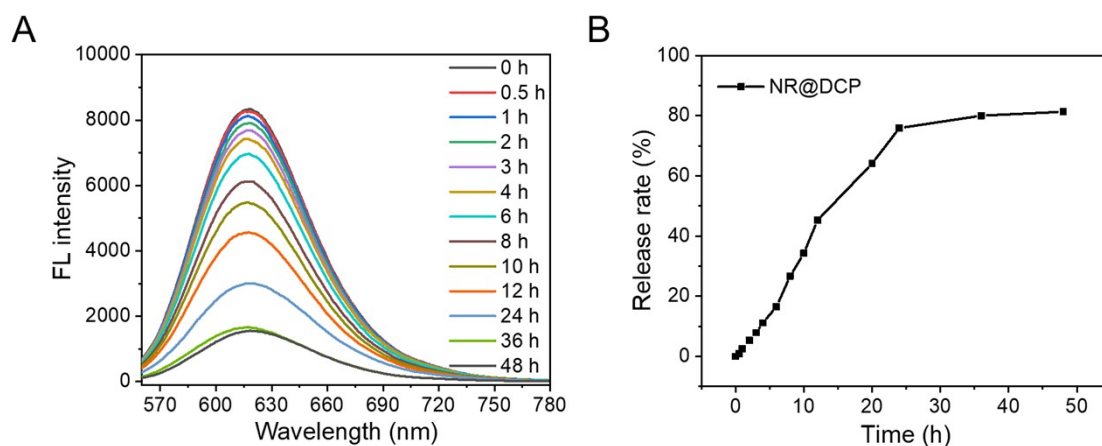


Fig. S10 Fluorescence spectra (A) and release rates (B) of NR-encapsulated DCP incubated with 10 mM GSH treatment for different time.

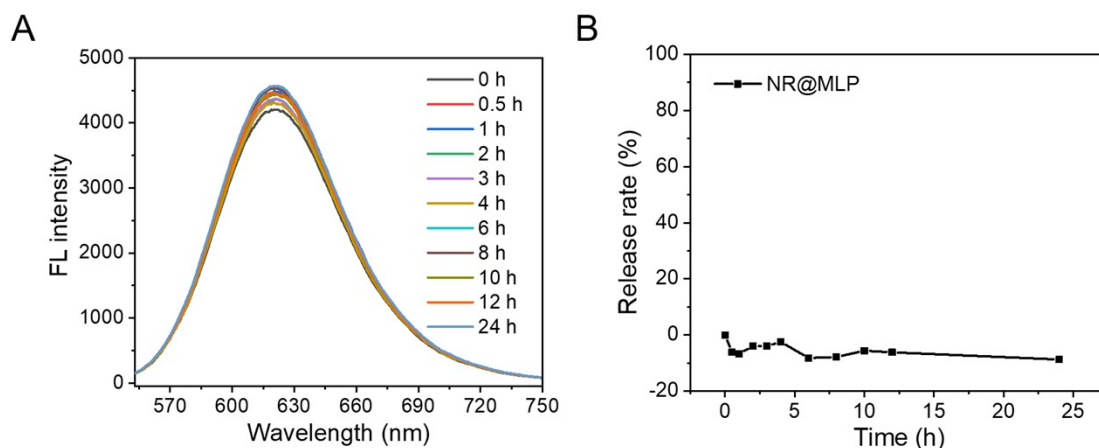


Fig. S11 Fluorescence spectra (A) and release rates (B) of NR-encapsulated MLP incubated with 10 mM GSH treatment for different time.

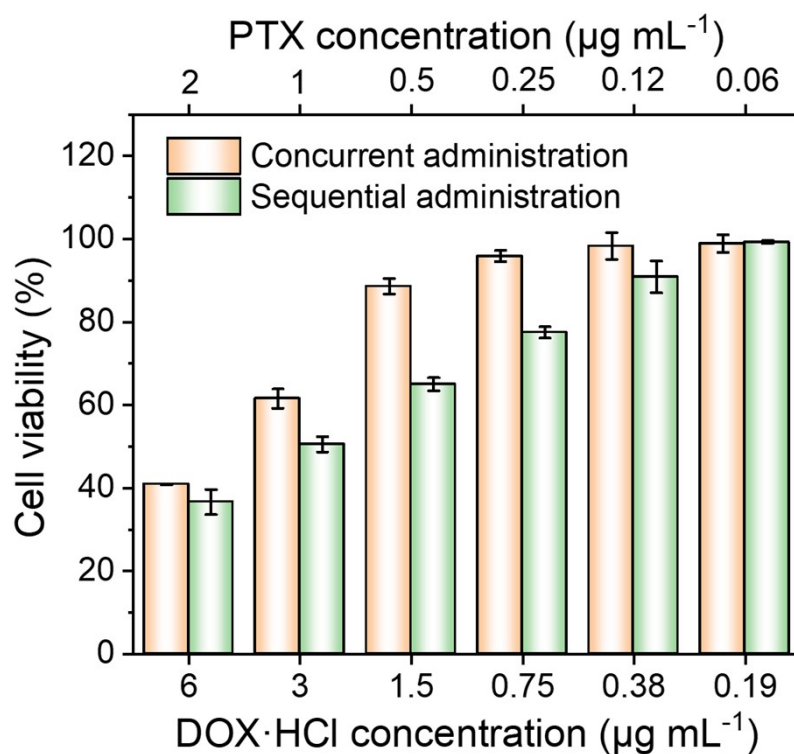


Fig. S12 Viability of GL261 cells incubated with DOX·HCl and PTX at different concentrations concurrently or sequentially.

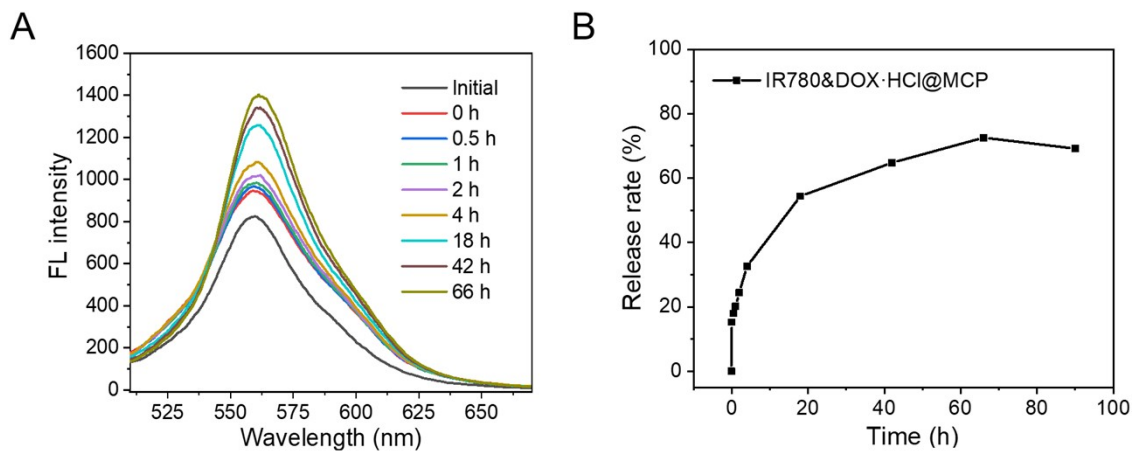


Fig. S13 Fluorescence spectra (A) and release rates (B) of IR780- and DOX·HCl-encapsulated MCP for different time after 5 min irradiation of 808 nm laser (2 W cm^{-2}).

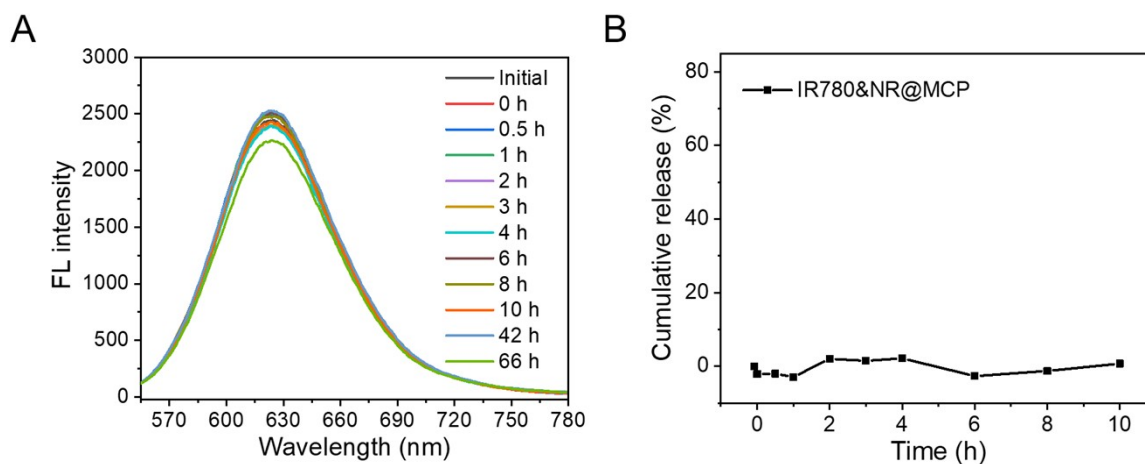


Fig. S14 Fluorescence spectra (A) and release rates (B) of IR780- and NR-encapsulated MCP for different time after 5 min irradiation of 808 nm laser (2 W cm^{-2}).

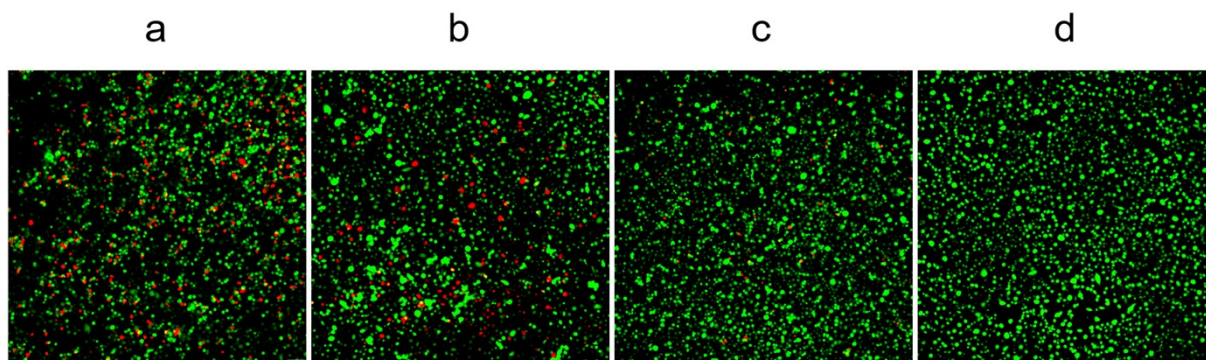


Fig. S15 Fluorescence stain of living and dead cells incubated for 24 h with drug-loaded vesicles (C_{IR780} : $0.335 \mu\text{g mL}^{-1}$, $C_{\text{DOX}\cdot\text{HCl}}$: $0.659 \mu\text{g mL}^{-1}$, C_{PTX} : $0.22 \mu\text{g mL}^{-1}$) after irradiation of 808 nm laser (2 W cm^{-2}) for 3 min. The live cells appeared green and the dead cells red in color. a: MCP; b: DCP; c: MLP; d: control. Scale bars: $75 \mu\text{m}$.

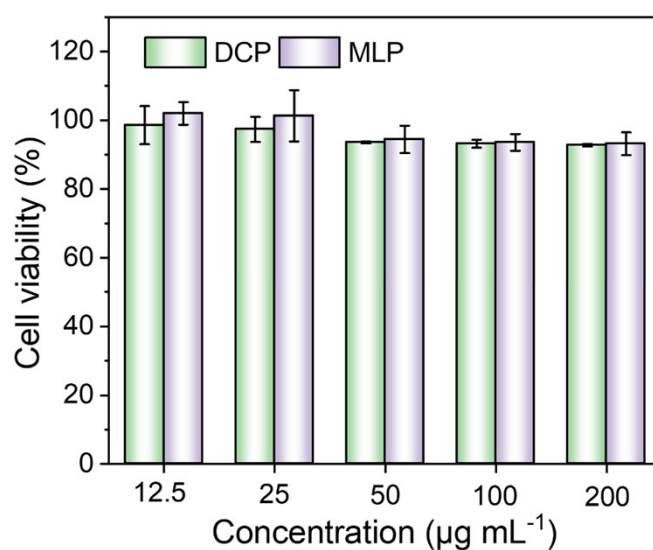


Fig. S16 Viability of 3T3 cells incubated with drug-free DCP and MLP at different concentrations for 24 h.

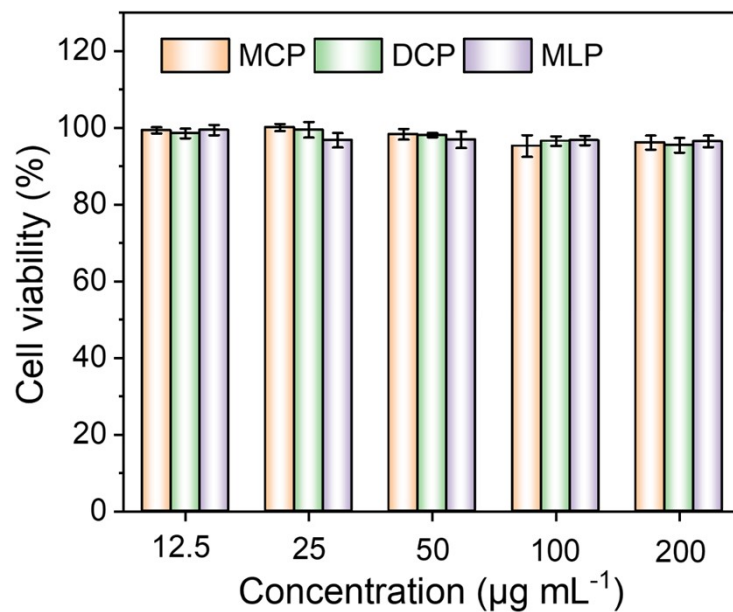


Fig. S17 Viability of GL261 cells incubated with drug-free MCP, DCP and MLP at different concentrations for 24 h.

Table S1. Hansen solubility parameter

Chemical structure	Solubility parameter
PCL	20.235
CDI	20.139
CDI-O	22.029
W	46.072
PEG	43.701

Table S2. DLS and SLS data of MCP and MCP-O vesicles

Samples ^a	Size (nm) ^b	PDI ^b	R_g (nm) ^c	R_h (nm) ^d	R_g/R_h
MCP	191.0	0.199	46.0	43.2	1.065
MCP-O	201.6	0.225	56.0	53.0	1.057

^a Multiblock copolymer vesicles before and after oxidation.

^b Size and PDI of the samples determined using a Zetasizer Nano ZS instrument (Malvern Instruments Ltd., UK) at an angle of 90°.

^c Radii of gyration from SLS measurement.

^d Mean hydrodynamic radii determined by DLS measurement.

Supporting reference

- 1 P. J. Hoogerbrugge and J. M. V. A. Koelman, *Europhys. Lett.*, 1992, **19**, 155-160.
- 2 P. Espanol and P. Warren, *Europhys. Lett.*, 1995, **30**, 191-196.
- 3 C. Junghans, M. Praprotnik and K. Kremer, *Soft Matter*, 2007, **4**, 156-161.
- 4 A. P. Thompson, H. M. Aktulga, R. Berger, D. S. Bolintineanu, W. M. Brown, P. S. Crozier, P. J. I. Veld, A. Kohlmeyer, S. G. Moore, T. D. Nguyen, R. Shan, M. J. Stevens, J. Tranchida, C. Trott and S. J. Plimpton, *Comput. Phys. Commun.*, 2022, **271**, 108171.
- 5 W. Humphrey, A. Dalke and K. Schulten, *J. Mol. Graphics*, 1996, **14**, 33-38.
- 6 A. D. Becke, *J. Chem. Phys.*, 1992, **96**, 2155-2160.
- 7 C. T. Lee, W. T. Yang and R. G. Parr, *Phys. Rev. B*, 1988, **37**, 785-789.
- 8 W. J. Hehre, R. Ditchfield and J. A. Pople, *J. Chem. Phys.*, 1972, **56**, 2257-2261.
- 9 A. V. Marenich, C. J. Cramer and D. G. Truhlar, *J. Phys. Chem. B*, 2009, **113**, 6378-6396.
- 10 F. Neese, *Comput. Mol. Sci.*, 2012, **2**, 73-78.